

# Charge separation in donor-C<sub>60</sub> complexes with real-time Green's functions: The importance of nonlocal correlations

E. Viñas Boström,<sup>1</sup> A. Mikkelsen,<sup>2</sup> C. Verdozzi,<sup>1</sup> E. Perfetto,<sup>3</sup> and G. Stefanucci<sup>4,5</sup>

<sup>1</sup>Lund University, Department of Physics and European Theoretical Spectroscopy Facility (ETSF), PO Box 118, 221 00 Lund, Sweden\*

<sup>2</sup>Lund University, Department of Physics and NanoLund, P.O. Box 118, 221 00 Lund, Sweden

<sup>3</sup>CNR-ISM, Division of Ultrafast Processes in Materials (FLASHit),

Area della Ricerca di Roma 1, Via Salaria Km 29.3, I-00016 Monterotondo Scalo, Italy

<sup>4</sup>Dipartimento di Fisica and European Theoretical Spectroscopy Facility (ETSF),

Università di Roma Tor Vergata, Via della Ricerca Scientifica 1, 00133 Rome, Italy

<sup>5</sup>INFN, Sezione di Roma Tor Vergata, Via della Ricerca Scientifica 1, 00133 Rome, Italy

We use the Nonequilibrium Green's Function (NEGF) method to perform real-time simulations of the ultrafast electron dynamics of photoexcited donor-C<sub>60</sub> complexes modeled by a Pariser-Parr-Pople Hamiltonian. The NEGF results are compared to mean-field Hartree-Fock (HF) calculations to disentangle the role of correlations. Initial benchmarking against numerically highly accurate time-dependent Density Matrix Renormalization Group calculations verifies the accuracy of NEGF. We then find that charge-transfer (CT) excitons partially decay into charge separated (CS) states if *dynamical* non-local correlation corrections are included. This CS process occurs in  $\sim 10$  fs after photoexcitation. In contrast, the probability of exciton recombination is almost 100% in HF simulations. These results are largely unaffected by nuclear vibrations; the latter become however essential whenever level misalignment hinders the CT process. The robust nature of our findings indicate that ultrafast CS driven by correlation-induced decoherence may occur in many organic nanoscale systems, but it will only be correctly predicted by theoretical treatments that include time-nonlocal correlations.

## I. INTRODUCTION

Charge separation (CS) after photoexcitation in nanoscale donor-acceptor (D-A) systems is the basic working principle of organic photovoltaics.<sup>1-3</sup> However, unraveling the mechanism responsible for the development of a CS state poses a formidable challenge since the formation and subsequent dissociation of the germinal charge-transfer (CT) exciton can occur through several competing (and system-dependent) channels, e.g., multiple CT excitons,<sup>4-8</sup> charge delocalization,<sup>9-14</sup> nuclear motion<sup>15-21</sup> and disorder<sup>22,23</sup>. To characterize these processes, donor-C<sub>60</sub> complexes have played an essential role as model systems and have been extensively studied both experimentally and theoretically<sup>24-28</sup>.

In particular, a variety of nanoscale donor systems have been coupled to C<sub>60</sub> such as carbon nanotubes, pentacene and a variety of organic complexes. Some of the mentioned studies indicated that very fast ( $< 100$  fs) exciton dissociation can occur<sup>27,28</sup> although, at the time, a direct experimental exploration of such ultrafast dynamics was not possible. This limitation has recently been overcome: experimental resolution of few tens of fs (or even less) is now readily available for surface studies, giving direct access to the sub 100 fs regime<sup>29-31</sup>. Even so, for a comprehensive interpretation of experiment, a comparison with numerical simulations of the electron and nuclear dynamics is needed.

Statistical approaches like Time-Dependent (TD) Density Functional Theory<sup>32-35</sup> (DFT) have been central in efforts to model charge transfer dynamics at the fs timescale. TD-DFT can in principle treat all electronic

excitations (Frenkel excitons, CT excitons, CS states, etc.) on equal footing through the Kohn-Sham equations for the electron density. The performance of TD-DFT crucially relies on the quality of the *exchange-correlation potential*, which is often approximated by a space- and time-local functional of the density. As we shall see, a time-local approximation is not always reliable.

An approach that includes in a natural way space-time nonlocal correlations is the NonEquilibrium Green's Function (NEGF) theory.<sup>36-38</sup> Here the accuracy of the results relies on the quality of the so called *correlation self-energy*  $\Sigma$ . If  $\Sigma = 0$  then NEGF is equivalent to the (time-local) TD Hartree-Fock (HF) theory. Since approximations to  $\Sigma$  can easily be generated and systematically improved by means of diagrammatic expansions, NEGF provides a natural framework to go beyond TD-HF, thus including space- and time-nonlocal correlation corrections to the electron dynamics.

In this work we highlight the crucial role that nonlocal correlations can have in the CS process of a prototypical D-A system. The NEGF method is initially benchmarked in a one-dimensional D-A model system against numerically accurate results from the TD Density Matrix Renormalization Group<sup>39,40</sup> (tDMRG), finding excellent agreement. In this assessment we also consider HF dynamics, as a paradigm of mean-field treatments, to help disentangle the role of correlations. Then, we consider a [HOMO+LUMO]-C<sub>60</sub> dyad modeled by a Pariser-Parr-Pople (PPP) Hamiltonian<sup>41,42</sup> with a single  $p_z$  orbital per Carbon, and show that the self-energy can qualitatively change the mean-field dynamics at clamped nuclei, from almost 100% recombination of the CT exciton in

HF to substantial CT and subsequent CS in correlated NEGF simulations. We find that the CS can happen already within 10 fs after the onset of photoexcitation. We further show that the results are largely unaffected by nuclear vibrations, which do instead play a pivotal role whenever the misalignment of the equilibrium levels prevents the formation of a CT exciton.

The paper is organized as follows: in Section II we describe the system and the inherent Hamiltonian. In Section III we present the theoretical approach; the choice of system parameters is discussed in Section IV; here an analysis of the possible choices for the initial state is also addressed. In Section V, we benchmark our Green's function approach against an exact solution for a paradigmatic 1D model. The role of electronic correlations for the donor-C<sub>60</sub> real-time dynamics is presented in Section VI. Finally, in Section VII the significance of the electron-phonon interactions is considered. Our conclusions and outlook are provided in Section VIII.

## II. DONOR-C<sub>60</sub> HAMILTONIAN

We consider a dyad consisting of a donor molecule coupled to a C<sub>60</sub> acceptor, see Fig. 1(a), with Hamiltonian

$$\hat{H}(t) = \hat{H}_d + \hat{H}_a + \hat{H}_{da} + \hat{H}_{e-ph} + \hat{H}_{ext}(t) \quad (1)$$

where  $\hat{H}_{d/a}$  describes the donor/acceptor molecule and  $\hat{H}_{da}$  the D-A coupling. The interaction with nuclear vibrations is contained in  $\hat{H}_{e-ph}$  whereas the interaction with external electromagnetic fields (the photoexcitation indicated in Fig. 1(a)) is accounted for by  $\hat{H}_{ext}(t)$ .

To facilitate the analysis we use a minimal paradigmatic description of the donor molecule, i.e., only two active orbitals (HOMO and LUMO) denoted by  $H$  and  $L$ :

$$\hat{H}_d = \epsilon_H \hat{n}_H + \epsilon_L \hat{n}_L + U_{HL} \hat{n}_H \hat{n}_L. \quad (2)$$

Here  $\epsilon_X$  is the energy of the  $X = H, L$  level,  $\hat{n}_X = \hat{n}_{X\uparrow} + \hat{n}_{X\downarrow} = \hat{c}_{X\uparrow}^\dagger \hat{c}_{X\uparrow} + \hat{c}_{X\downarrow}^\dagger \hat{c}_{X\downarrow}$  is the occupation operator of the same level and  $U_{HL}$  is the Coulomb interaction between electrons on different levels. For the C<sub>60</sub> acceptor we use a single  $p_z$ -orbital per carbon and write

$$\begin{aligned} \hat{H}_a = & - \sum_{ij\sigma} t_{ij} \left( \hat{c}_{i\sigma}^\dagger \hat{c}_{j\sigma} + h.c. \right) + \sum_i V \hat{n}_{i\uparrow} \hat{n}_{i\downarrow}, \\ & + \sum_{i \neq j} \lambda V \frac{\hat{n}_i \hat{n}_j}{\sqrt{\lambda^2 + d_{ij}^2}} \end{aligned} \quad (3)$$

where  $t_{ij}$  and  $d_{ij}$  are, respectively, the hopping amplitude and the distance between carbons  $i$  and  $j$ . We take  $t_{ij} = t$  for two atoms belonging to the same pentagon and  $t_{ij} = t'$  for two atoms in different pentagons. In Ohno's parametrization<sup>43</sup> of the interaction (last term of Eq. (3))  $\lambda$  accounts for the screening from the frozen shells.

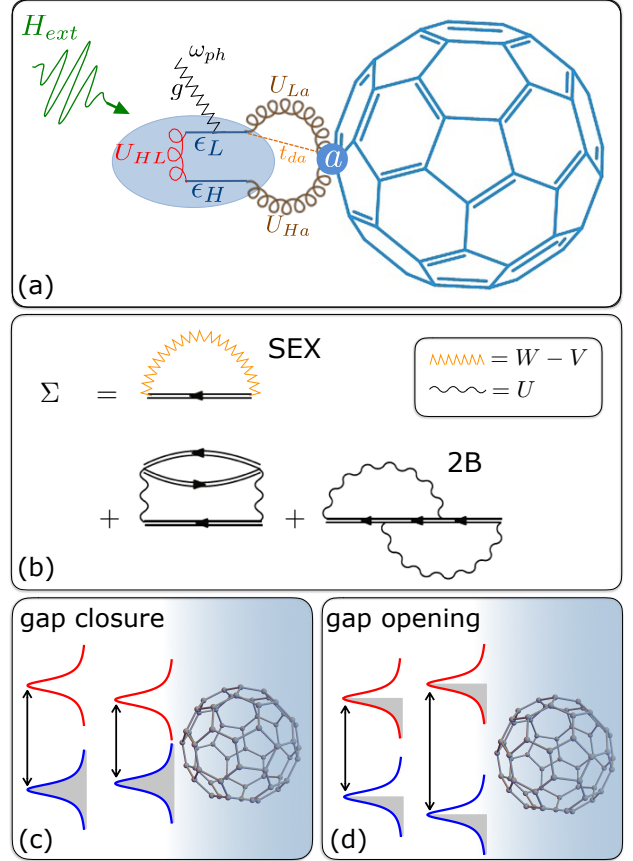


FIG. 1: (a) Sketch of the model and experiment. The nomenclature used for the terms in the Hamiltonian is also shown. (b) Self-energy approximation consisting of the SEX diagram (first term) and the 2B diagrams (second and third term). Gap closure for a filled HOMO and empty LUMO (c) and gap opening for a half-filled HOMO and LUMO (d) due to polarization effects induced by C<sub>60</sub> (or any polarizable molecule or surface).

We consider a donor with the HOMO orbital located far enough from the C<sub>60</sub>  $p_z$ -orbitals that we can neglect their overlaps. The LUMO orbital is instead located in the neighbourhood of the acceptor and has a substantial overlap with only one  $p_z$ -orbital (labelled by the index  $i = 1$ ); let  $t_{da}$  be the corresponding hopping integral. Accordingly, the Hamiltonian for the D-A interaction is described by

$$\begin{aligned} H_{da} = & -t_{da} \sum_{\sigma} \left( \hat{c}_{L\sigma}^\dagger \hat{c}_{1\sigma} + h.c. \right) \\ & + \sum_i [U_{Hi} (\hat{n}_H - 2) + U_{Li} \hat{n}_L] (\hat{n}_i - 1), \end{aligned} \quad (4)$$

where  $U_{Xi}$  is the strength of the Coulomb repulsion between an electron on  $X = H, L$  and an electron on carbon  $i$ <sup>44,45</sup>. The interaction correctly vanishes in the charge neutral ground state (2 electrons on the HOMO and 1 electron per C atom on the C<sub>60</sub>) of the subsystems D

and A at infinite distance ( $t_{da} = 0$ ). The index  $i$  could in principle run across all the 60 atoms of the acceptor. In the actual calculations we considered only atom  $i = 1$  and its nearest neighbors.

To demonstrate the robustness of the correlated results we also investigate the effects of harmonic nuclear motion on the electron dynamics. We model the electron-phonon interaction as

$$\hat{H}_{e-ph} = \frac{p^2}{2M} + \frac{1}{2}M\omega_{ph}^2 x^2 + g\hat{n}_L x, \quad (5)$$

which describes a Holstein-like phonon<sup>46</sup> coupled to the charge density of the LUMO level.

An external light field is used to promote an electron from the HOMO to the LUMO level. We therefore restrict the light-matter interaction to the donor site

$$\hat{H}_{ext}(t) = 2A \cos(\omega t) \sum_{\sigma} \left( \hat{c}_{H\sigma}^{\dagger} \hat{c}_{L\sigma} + h.c. \right). \quad (6)$$

The action of  $\hat{H}_{ext}$  starts at  $t = 0$  and ends at some time  $t_{off}$  when the LUMO population (initially zero) has become close to unity. In this work we consider a frequency  $\omega = \epsilon_L - \epsilon_H$  close to resonant absorption.

### III. METHOD

As the  $p_z$ -orbitals are half-filled we use the statically screened exchange (SEX) approximation to treat the bare interaction  $V_{ij} = \lambda V / \sqrt{\lambda^2 + d_{ij}^2}$  on the  $C_{60}$ .<sup>1</sup> Thus, the first contribution to  $\Sigma$  is given by the first diagram in Fig. 1(b) where (in matrix notation)

$$W = \frac{V}{1 - V\chi_0}, \quad (7)$$

and  $\chi_0$  is the zero-frequency response function<sup>37</sup>

$$\chi_{0,ij} = 2 \sum_{n\bar{n}} \frac{\phi_n(i)\phi_{\bar{n}}(i)\phi_n(j)\phi_{\bar{n}}(j)}{\epsilon_n - \epsilon_{\bar{n}}}. \quad (8)$$

In Eq. (8)  $\phi_n$  and  $\epsilon_n$  are the HF orbitals and energies of the isolated  $C_{60}$ , and the indices  $n$  and  $\bar{n}$  run over occupied and unoccupied states respectively. We emphasize that the screening described by  $W$  comes solely from the valence electrons and it is therefore of different physical origin than that described by  $\lambda$  (which is due to the frozen electrons not included explicitly in our description). Hence, no double counting is involved.

<sup>1</sup> Our treatment corresponds to the static Coulomb hole plus screened exchange (COH-SEX) approximation first introduced by Hedin<sup>47</sup>. However, the Coulomb hole part only gives a constant shift of the diagonal of the self-energy, that can be absorbed by redefining the single-particle energies.

The electron-hole attraction experienced by the CT exciton is responsible for the renormalization of the HOMO-LUMO gap, an effect missed by HF and even by Hartree+SEX. The gap tends to close in equilibrium (filled HOMO and empty LUMO), see Fig 1(c), whereas it tends to open in the photoexcited donor (half-filled HOMO and LUMO), see Fig 1(d) and Supporting Information. The gap closure in the equilibrium case is of relevance in, e.g., estimating the conductance of a molecular junction.<sup>44,45,48,49</sup> The gap opening in the photoexcited case is instead of relevance to CS since the formation of a CT exciton strongly depends upon level alignment. Both types of gap renormalization are captured by the second-Born (2B) approximation to the self-energy. We therefore add to the SEX diagram the last two diagrams in Fig. 1(b) where  $U$  is the interaction in Eqs. (2) and (4).

In the NEGF method the total self-energy  $\Sigma$  is used to generate the so called Kadanoff-Baym equations<sup>36-38,50-55</sup> (KBE) for the Green's function. The KBE are subsequently converted into an integro-differential equation for the single-particle density matrix using the Generalized Kadanoff-Baym Ansatz<sup>56,57</sup> (GKBA), which has proven to drastically reduce the computational cost without loosing accuracy<sup>58,59</sup> and it has recently been implemented in the context of quantum transport,<sup>60</sup> equilibrium absorption,<sup>61</sup> transient absorption,<sup>62-65</sup> carrier dynamics in semiconductors<sup>66,67</sup> and many-body localization.<sup>68,69</sup> The derivation of the GKBA equation is provided in the Supporting Information.

As for the effects of nuclear vibrations we use a NEGF-Ehrenfest approximation,<sup>70,71</sup> i.e., we replace the momentum and position operators with their expectation values in the GKBA equation and evolve the nuclear degrees of freedom via the Ehrenfest dynamics.

### IV. ON THE INITIAL STATE

In accordance with the literature<sup>72-74</sup> the values of the hopping integrals have been set to  $t = 2.5$  eV and  $t' = 2.7$  eV. The strength of the interaction on the  $C_{60}$  takes the value  $V = 8$  eV with  $\lambda = 0.7$  Å<sup>73,74</sup>. The D-A coupling is smaller than the  $C_{60}$  parameters since no chemical bond is formed between the molecules. We have found that in this regime, i.e. as long as  $t_{da}$  is the smallest energy scale in the system, the results do not change qualitatively for different couplings. In the following we set the hopping integral  $t_{da} = 0.4$  eV. The D-A interaction strength is taken as  $U_{Li} = U_{La}$  and  $U_{Hi} = U_{Ha}$  for  $i = 1$ ,  $U_{Li} = U_{La}/2$  and  $U_{Hi} = U_{Ha}/2$  for the nearest neighbours of  $i = 1$  and zero otherwise, where  $U_{La} = 2U_{Ha} = 2$  eV ( $U_{La} > U_{Ha}$  since the HOMO is further away than the LUMO from the  $C_{60}$ ). The bare energies of the HOMO and LUMO levels are  $\epsilon_H = -2.4$  eV,  $\epsilon_L = 0.6$  eV whereas the HOMO-LUMO repulsion is  $U_{HL} = 1$  eV. Unless explicitly stated, all results refer

to this set of parameter values. The resulting *equilibrium* HF density of states is shown in Fig. 2 (top panel), and is in good qualitative agreement with both experiment and other theoretical results<sup>75–77</sup>.

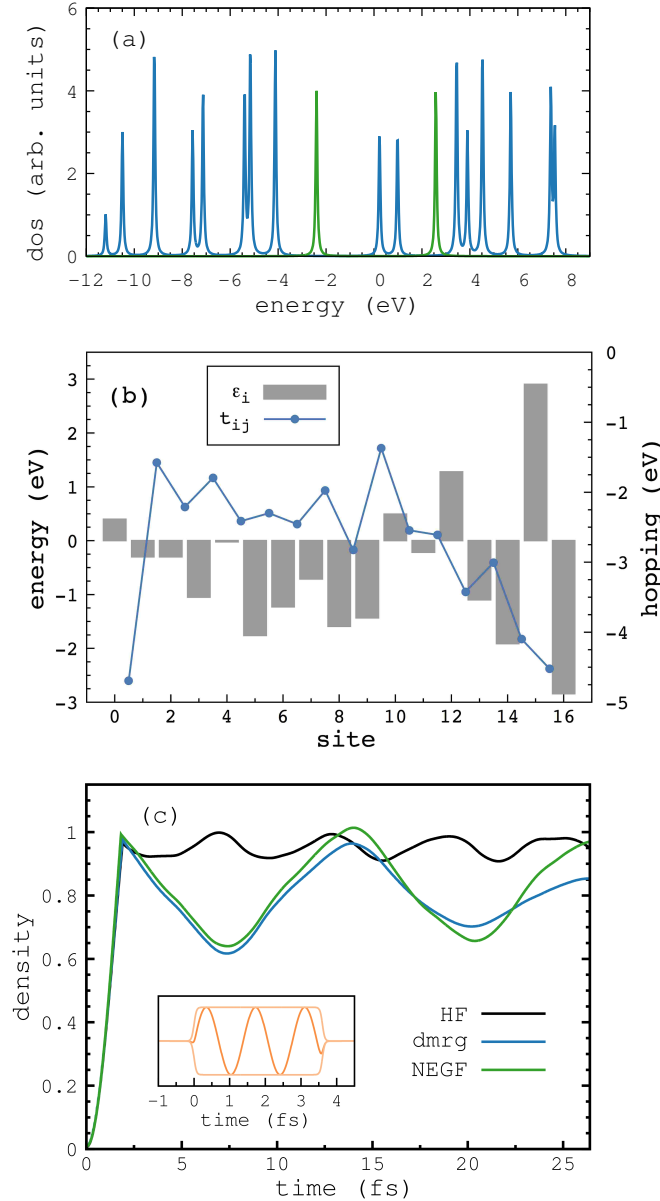


FIG. 2: (a) HF Density of states for the coupled donor- $C_{60}$  system, with blue peaks denoting  $C_{60}$  levels and green peaks the HOMO and LUMO of the donor. (b) Parameters of the one-dimensional Lanczos chain of the noninteracting  $C_{60}$ . Gray bars indicate the values of the onsite energies  $\epsilon_i$  whereas blue dots the nearest neighbour hopping integrals  $t_{ij}$ . (c) Electron occupation of the LUMO level for the donor coupled to the Lanczos chain using HF, NEGF and tDMRG. The inset shows the profile of the laser pulse along with its rectangular envelope.

The first step in a CT process is the photoexcitation of the electron from the initially occupied HOMO. Due to absence of spin symmetry breaking terms, the occu-

pations  $n_{X\sigma}$  ( $X = H, L$ ) remain independent of  $\sigma$  during the entire time evolution. In photoemission a common way of treating the photoexcitation is to employ the sudden approximation<sup>78</sup>, wherein the HOMO hole is assumed to be created instantaneously. The rationale behind this approximation is that the time it takes for the electron to escape can be made arbitrarily short by using photons of high frequency. The sudden approximation applied to the HOMO-LUMO transition would yield the initial state  $|\Psi_\sigma^{(1)}\rangle = \hat{c}_{L\sigma}^\dagger \hat{c}_{H\sigma} |\Psi_0\rangle$ , where  $|\Psi_0\rangle$  is the ground state of the system. However, for the HOMO-LUMO transition, the time to transfer an electron is ultimately bounded by the inverse of the Rabi frequency. From the exact solution of the two-level system driven by the perturbation in Eq. (6) one finds that the state with a half-filled HOMO and LUMO reads  $|\Psi^{(2)}\rangle = \frac{1}{4} (\hat{c}_{L\downarrow}^\dagger - i\hat{c}_{H\downarrow}^\dagger) \hat{c}_{H\downarrow} (\hat{c}_{L\uparrow}^\dagger - i\hat{c}_{H\uparrow}^\dagger) \hat{c}_{H\uparrow} |\Psi_0\rangle$ . We thus see that  $|\Psi^{(2)}\rangle$  is a linear combination of the ground state  $|\Psi_0\rangle$ , the singly excited states  $|\Psi_\sigma^{(1)}\rangle$  and the doubly excited state  $\hat{c}_{L\downarrow}^\dagger \hat{c}_{H\downarrow} \hat{c}_{L\uparrow}^\dagger \hat{c}_{H\uparrow} |\Psi_0\rangle$ . We have compared the dynamics obtained using  $|\Psi_\sigma^{(1)}\rangle$  and  $|\Psi^{(2)}\rangle$  as initial states, as well as direct excitation using an external field, and found scenarios where the sudden approximation fails dramatically. In this paper we exclusively use an external field to initiate the dynamics. We take the amplitude in Eq. (6) to be  $A = 0.3$  eV, which given a typical HOMO-LUMO dipole  $d = 1 \div 10$  a.u. corresponds to a laser intensity of  $I = 4.2 \times (10^{10} \div 10^{12})$  W/cm<sup>2</sup>. A discussion on the dependence of the excitation pulse and on the differences with the sudden approximation is given in the Supporting Information.

## V. BENCHMARKS WITH TDMRG

The accuracy of NEGF results is discussed in this Section by direct comparison with tDMRG on a simplified system. Since tDMRG is a numerically highly accurate scheme for one-dimensional models, we map the donor- $C_{60}$  Hamiltonian onto a linear chain. For the noninteracting  $C_{60}$  this is achieved using the Lanczos method<sup>79</sup>, and results in a 17 site chain with different nearest neighbor hopping and on-site energies<sup>2</sup>. The parameters of the Lanczos chain are shown in Fig. 2 (middle panel). We then include interactions between the LUMO level and the first site of the chain (tDMRG is most effective for short-range interactions) of strength  $U_{La} = 0.8$  (here  $U_{Ha} = 0$ ).

We perform TD simulations for the monochromatic driving of Eq. (6) switched on approximately in the time

<sup>2</sup> Use of the Lanczos technique to reformulate a problem via a 1D effective Hamiltonian, is a quite common procedure, notably in theoretical surface science. For a recent application in quantum transport, see e.g. [80]

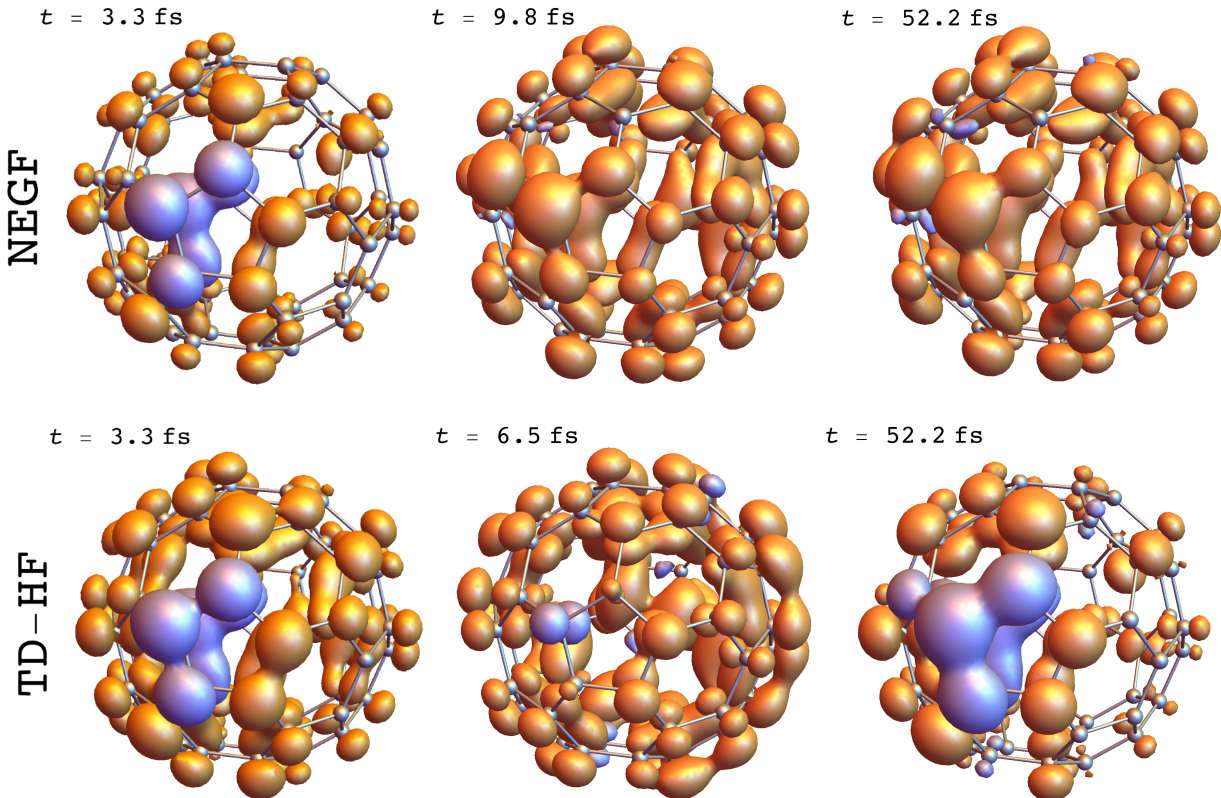


FIG. 3: Charge dynamics in NEGF (upper row) and TD-HF (lower row) for the  $C_{60}$  acceptor. In each row, the three time snapshots depict the excess density as defined in Eq. (9) (blue for  $\Delta n < 0$  and orange for  $\Delta n > 0$ ). With reference to Fig. 4a–b, they respectively correspond to the time of maximum photo-charging of the LUMO ( $t = 3.26$  fs), the first time the LUMO reaches minimum density (at  $t = 9.78$  fs for NEGF and  $t = 6.52$  fs in TD-HF) and its later occupation at  $t = 52.16$  fs.

window  $(0, \pi/3A)$  using HF, NEGF and tDMRG. The results for the TD occupation of the LUMO are shown in Fig. 2 (bottom panel) and we see that the NEGF dynamics agrees very well with the tDMRG one. The HF results on the other hand are qualitatively different, and show almost no dynamics for the LUMO density.

## VI. DONOR- $C_{60}$ REAL-TIME DYNAMICS

In this Section we discuss real-time simulations of the electron dynamics of the full donor- $C_{60}$  system driven out of equilibrium by the external field in Eq. (6) switched on between  $t = 0$  and approximately  $t = \pi/(3A)$ . This corresponds to a duration of about 3 fs and a pumping of about one electron from HOMO to LUMO. The NEGF results are shown in Fig. 3 and Fig. 4, where HF calculations are also reported for comparison. In Fig. 3 we display three snapshots of the excess electron density

$$\Delta n(\mathbf{r}, t) = \sum_{ij} [\rho_{ij}(t) - \rho_{ij}(0)] \varphi_i^*(\mathbf{r}) \varphi_j(\mathbf{r}) \quad (9)$$

where  $\varphi_i$  is the  $p_z$ -orbital of carbon  $i$ . Compared to the ground (initial) state density at  $t = 0$ , large orange (blue)

regions indicate regions of higher (lower) electron density at time  $t$ , i.e.  $\Delta n(\mathbf{r}, t) > 0$  ( $\Delta n(\mathbf{r}, t) < 0$ ).

In Figs. 4c and 4d we show the excess density *per shell*, where the shells are defined according to their proximity to the LUMO (hence the first shell consists only of atom 1). For better visualization each shell is given a different color. The shell geometric position is indicated in the small  $C_{60}$  model in the Figure.

We now go on to describe the excitation process. The action of the external field (photoexcitation) fills the LUMO level of the donor during the first 3 fs (as seen in Fig. 4a–b). This coincides with a depletion of electrons in the shells of the  $C_{60}$  closest to the donor atom as seen in Fig. 3. This is an image charge effect reflecting the increased interaction felt by the electrons on the  $C_{60}$  due to the additional LUMO charge. Once the pumping is over the charge on the LUMO flows into the  $C_{60}$ , thus forming a CT exciton (excess of charge at the interface shells). This is indicated by the minimum in the LUMO occupation at 9.8 fs for NEGF and 6.5 fs for HF calculations (see again Fig. 4a–b) and the corresponding charge distribution change in the  $C_{60}$  is shown in the middle images of Fig. 3. During this action of the external field and shortly after the end of it, i.e., up until the formation of the CT exciton, the charge dynamics in TD-HF

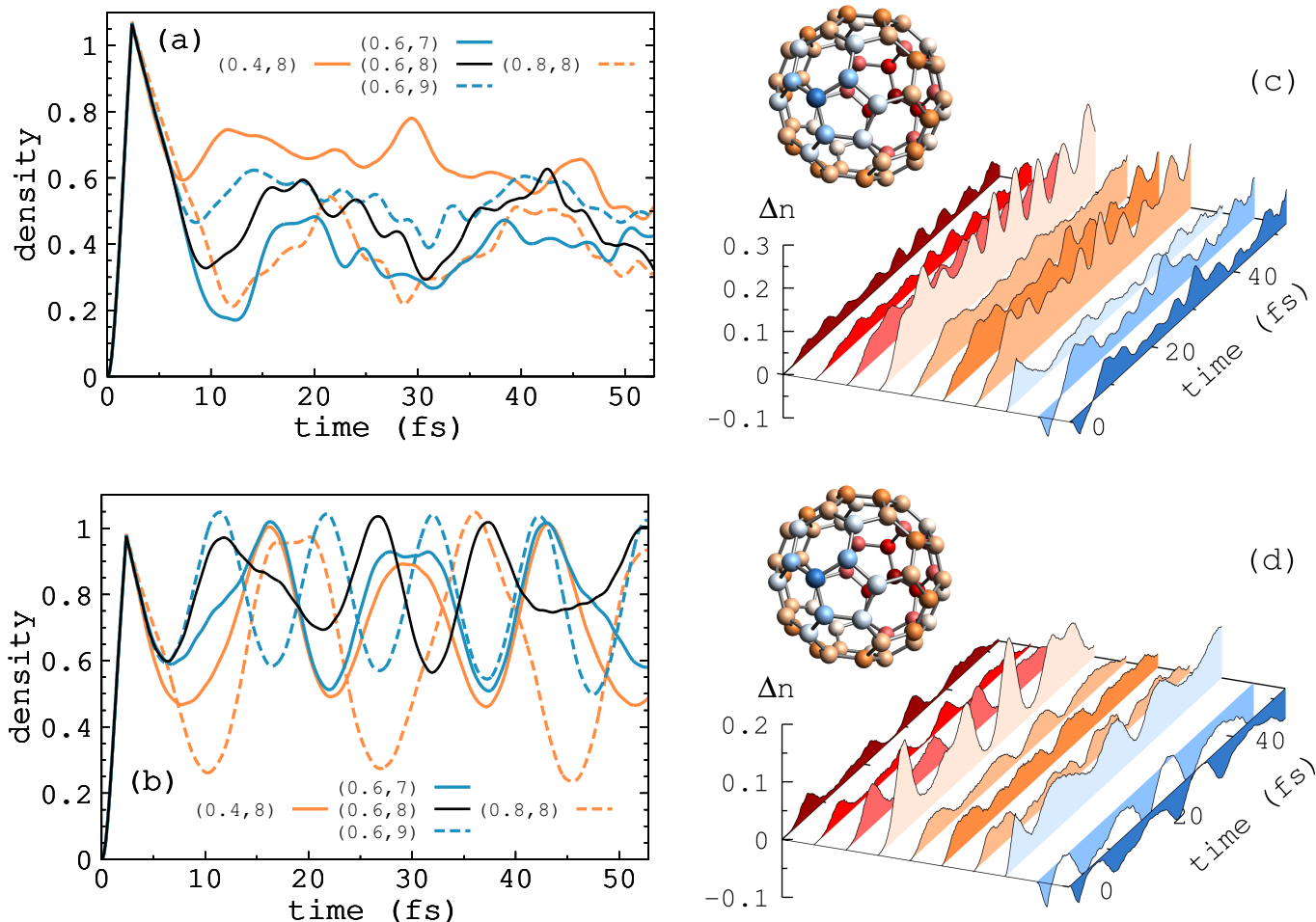


FIG. 4: NEGF (a) and TD-HF (b) results for the LUMO density for different values (in units of eV) of  $(\epsilon_L, V) = (0.4, 8)$ ,  $(0.6, 7)$ ,  $(0.6, 8)$ ,  $(0.6, 9)$ ,  $(0.8, 8)$  [the default parameters  $(\epsilon_L, V) = (0.6, 8)$  give the black curve]. The excess density in the  $C_{60}$  shells as a function of time is shown in panels (c) and (d) for NEGF and TD-HF, respectively. Atoms of the same shells have the same color, as indicated in the  $C_{60}$  cluster.

has many features in common with NEGF, see Fig. 4. However, at this point the two models strongly diverge.

In the case of NEGF, the charge spreads over the entire molecule and stabilizes on the central shells, as it can be seen in Fig. 4c. Even though there are still oscillations in the charge density at the end of the simulation, the average charge on the LUMO is between 0.5-0.3 – much less than unity (see Fig. 4a). This indicates that the CT exciton has partially decayed into a CS state. Interestingly, we note that the majority of charge is transferred in less than 10 fs and for all model parameters the density has stabilised within 50 fs.

In contrast, in TD-HF the system does not evolve toward a CS state: the LUMO occupation periodically returns to the value reached just after the photoexcitation, as seen in Fig. 4b. From Fig. 4d we see that the charge oscillates back and forth through the molecule with a period slightly longer than  $\simeq 10$  fs. The difference can also quite strikingly be seen in Fig. 3 where, after 52 fs, the TD-HF distribution has returned to a situation very

closely resembling that after 3 fs and the NEGF distribution has settled in a new state.

Similar scenarios are observed for a range of parameters around the values introduced in Section IV, see Fig. 4(a-b). Although the amount of charge transferred from the donor to the  $C_{60}$  may vary, the system always evolves toward a CS state in NEGF whereas it bounces back to the initial state in TD-HF.

The results presented in this Section point to the possibility of obtaining a CS state driven by correlation-induced decoherence. This process would occur in a few tens of fs. Experimental indications of such ultrafast processes have been observed<sup>27,28</sup>, although the explanations were somewhat different. In the NEGF language, capturing a mechanism based on correlation-induced decoherence requires a space-time nonlocal self-energy. It is therefore out of reach of TD-HF or any other time-local theory like e.g. TD-DFT with adiabatic functionals.

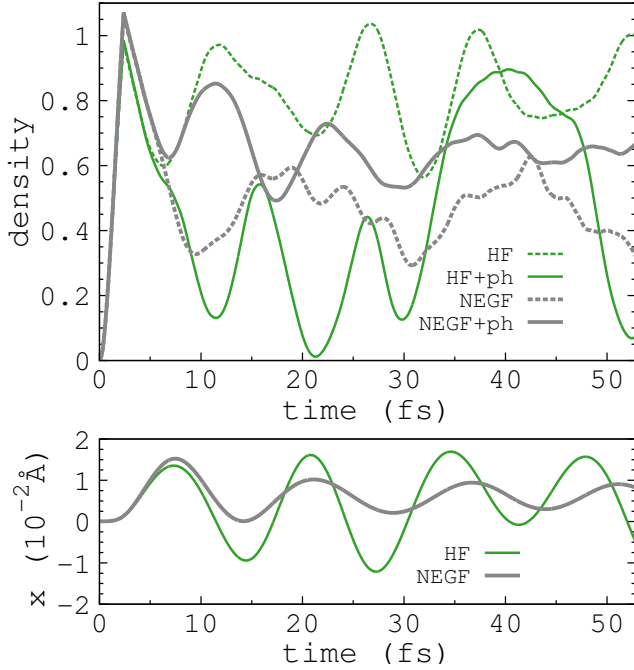


FIG. 5: LUMO occupation (top) and nuclear coordinate (bottom) for a donor- $C_{60}$  system with electron-phonon coupling. In the initial state the LUMO and  $C_{60}$  levels are partially aligned. Results are shown for HF (green-solid) and NEGF (grey-solid). For better comparison we also show results without electron-phonon coupling (dashed).

## VII. ELECTRON-PHONON DYNAMICS

We here address the effects of a single nuclear vibration of the Holstein<sup>46</sup> (local) type coupled to the LUMO density as in Eq. (5). The photo-induced oscillations of the coordinate  $x$  renormalizes the energy levels, in agreement with the physical picture obtained using TD-DFT.<sup>15,16</sup>

We show in Fig. 5 results for the same parameters as in Figs. 3 and 4 with  $\omega_{ph} = 0.548$  eV,  $g = 20$  eV/Å and  $M$  about forty times the proton mass. The NEGF dynamics is largely unaffected by the nuclear vibration, the only change being a slight decrease in the charge transferred. The Holstein mode changes quantitatively the TD-HF behavior but there is still no clear evidence of CS.

It is interesting to explore a different regime where, at clamped nuclei, due to level misalignment there is no CT either in NEGF nor in TD-HF. For this purpose we change the donor parameters and consider  $\epsilon_H = -1.4$  eV,  $\epsilon_L = 1.6$  eV,  $U_{HL} = 0.6$  eV and  $U_{La} = 2U_{Ha} = 1.2$  eV. The results are shown by the dashed curves in Fig. 6. When the coupling to the nuclear vibration is turned on, with  $\omega_{ph}$ ,  $g$  and  $M$  as before, a dramatic change in the CT behavior is observed. The TD-HF calculations go from showing almost vanishing CT to efficient CS. A similar regime with analogous findings has been investigated by other authors using adiabatic TD-DFT<sup>15,16</sup>. We also notice that space-time nonlocal electronic cor-

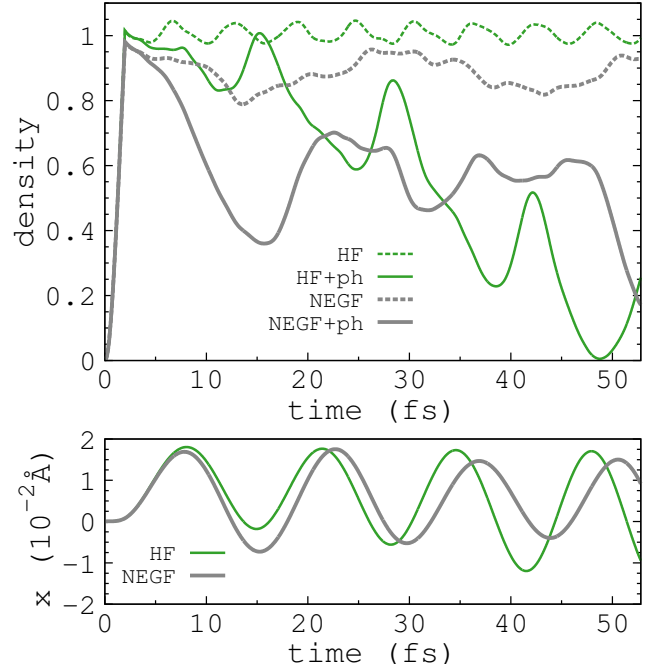


FIG. 6: LUMO occupation (top) and nuclear coordinate (bottom) for a donor- $C_{60}$  system with electron-phonon coupling and modified donor parameters, see main text. In the initial state the LUMO and  $C_{60}$  levels are misaligned. Results are shown for HF (green-solid) and NEGF (grey-solid). For better comparison we also show results without electron-phonon coupling (dashed).

relations (NEGF results) do not change the qualitative picture, the main effect being a less efficient CS. This can easily be understood in terms of quasi-particles. In HF the quasi-particles have an infinitely long life-time or, equivalently, a sharp energy. Therefore, when the phonon-shifted HF LUMO energy aligns to an unoccupied acceptor level the CT is extremely efficient. Beyond HF the quasiparticle weight spread over several energies and CT occurs whenever the donor and acceptor spectral densities overlap. As this overlap is always smaller than unity only a fraction of the electron charge can be transferred.

The reported evidence is based on simulations with Holstein-like phonons. However, we performed calculations with Fröhlich-like phonons as well (not shown), i.e., we replaced the coupling  $g \hat{n}_L x$  with  $g \sum_{\sigma} (\hat{c}_{L\sigma}^{\dagger} \hat{c}_{1\sigma} + h.c.)x$ , arriving at similar conclusions.

## VIII. CONCLUSIONS AND OUTLOOK

We performed real-time NEGF simulations of the charge dynamics in a donor- $C_{60}$  dyad photoexcited by external laser pulses. The accuracy of the NEGF scheme was preliminary assessed through comparison with tDMRG data in D-A one-dimensional model systems, finding excellent agreement.

We reported results for two different physical situations, namely levels alignment allowing and forbidding the formation of a CT exciton. In the former case we find that the CT exciton dissociates and the system evolves toward a CS state even with clamped nuclei. We highlighted the role of space-time nonlocal correlations (or, equivalently, correlation-induced decoherence) by comparing NEGF and TD-HF. In TD-HF the CT exciton recombines and no evidence of CS is observed. We also verified that the inclusion of nuclear motion does not change the picture. However, in the second physical situation, i.e., level alignment forbidding CT, we find that the impact of nuclear motion is substantial. In fact, both TD-HF and NEGF predict CS due to coupling to nuclear vibrations, albeit in NEGF the yield of exciton dissociation is smaller. The TD-HF results agree with similar findings in organic D–A complexes obtained using TD–DFT.<sup>15,16</sup>

Although we focused on a C<sub>60</sub> acceptor, the NEGF method can also be used to deal with donors and adsorbates on surfaces, as it has been already demonstrated in the context of molecular electronics.<sup>81,82</sup> In these instances, the only approximation is that one should cut off the Coulomb interaction in the self-energy diagrams to a finite region in the neighbourhood of the donor or the adsorbate species. In a broader perspective, our results put forward NEGF as a well suited tool for an accu-

rate description of general time-dependent electronic phenomena, in particular to characterise how nonlocal correlations influence realistic nanostructured systems and surfaces, also when nuclear degrees of freedom are involved. This might be particularly important for studies of electron dynamics in the first hundred femtoseconds after excitation – an area which has become accessible to experimental studies in recent years, and which has a strong influence on the dynamical properties of for example nanoscale solar harvesting systems, optoelectronic components, surface-induced molecular dissociation/synthesis and desorption phenomena.<sup>83</sup>

## IX. ACKNOWLEDGEMENTS

A. M. was supported by the Swedish Research Council (VR). E.P. acknowledges funding from the European Union project MaX Materials design at the exascale H2020-EINFRA-2015-1, Grant Agreement No. 676598 and Nanoscience Foundries and Fine Analysis-Europe H2020-INFRAIA-2014-2015, Grant Agreement No. 654360. G.S. acknowledges funding by MIUR FIRB Grant No. RBFR12SW0J and EC funding through the RISE Co-ExAN (GA644076).

\* Electronic address: emil.bostrom@teorfys.lu.se

- <sup>1</sup> F. Gao and O. Inganäs, *Phys. Chem. Chem. Phys.* **16**, 20291 (2014).
- <sup>2</sup> P. Song, Y. Li, F. Ma, T. Pullerits, and M. Sun, *The Chemical Record* **16**, 734 (2016).
- <sup>3</sup> C. A. Rozzi, F. Troiani, and I. Tavernelli, arXiv:1706.06656 (2017).
- <sup>4</sup> S. D. Dimitrov, A. A. Bakulin, C. B. Nielsen, B. C. Schroeder, J. Du, H. Bronstein, I. McCulloch, R. H. Friend, and J. R. Durrant, *Journal of the American Chemical Society* **134**, 18189 (2012).
- <sup>5</sup> G. Grancini, M. Maiuri, D. Fazzi, A. Petrozza, H.-J. Egelhaaf, D. Brida, G. Cerullo, and G. Lanzani, *Nat. Mater.* **12**, 29 (2013).
- <sup>6</sup> B. M. Savoie, A. Rao, A. A. Bakulin, S. Gelinas, B. Movaghar, R. H. Friend, T. J. Marks, and M. A. Ratner, *Journal of the American Chemical Society* **136**, 2876 (2014).
- <sup>7</sup> H. Ma and A. Troisi, *The Journal of Physical Chemistry C* **118**, 27272 (2014).
- <sup>8</sup> G. Wu, Z. Li, X. Zhang, and G. Lu, *The Journal of Physical Chemistry Letters* **5**, 2649 (2014).
- <sup>9</sup> A. A. Bakulin, A. Rao, V. G. Pavelyev, P. H. M. van Loosdrecht, M. S. Pshenichnikov, D. Niedzialek, J. Cornil, D. Beljonne, and R. H. Friend, *Science* **335**, 1340 (2012).
- <sup>10</sup> D. Caruso and A. Troisi, *Proceedings of the National Academy of Sciences* **109**, 13498 (2012).
- <sup>11</sup> H. Tamura and I. Burghardt, *Journal of the American Chemical Society* **135**, 16364 (2013).
- <sup>12</sup> M. Huix-Rotllant, H. Tamura, and I. Burghardt, *The Jour-*

- nal of Physical Chemistry Letters* **6**, 1702 (2015).
- <sup>13</sup> F. Gao, W. Tress, J. Wang, and O. Inganäs, *Phys. Rev. Lett.* **114**, 128701 (2015).
- <sup>14</sup> G. D’Avino, L. Muccioli, Y. Olivier, and D. Beljonne, *The Journal of Physical Chemistry Letters* **7**, 536 (2016).
- <sup>15</sup> C. A. Rozzi, S. M. Falke, N. Spallanzani, R. Angel, E. Molinari, D. Brida, M. Maiuri, H. Cerullo, G. Schramm, J. Christoffers, and C. Lienau, *Nature Communications* **4** (2013).
- <sup>16</sup> S. M. Falke, C. A. Rozzi, D. Brida, M. Maiuri, M. Amato, E. Sommer, A. De Sio, A. Rubio, G. Cerullo, E. Molinari, et al., *Science* **344**, 1001 (2014).
- <sup>17</sup> Y. Song, S. N. Clifton, R. D. Pensack, T. W. Kee, and G. D. Scholes, *Nature Communications* **5**, 4933 (2014).
- <sup>18</sup> Y. Xie, J. Zheng, and Z. Lan, *The Journal of Chemical Physics* **142**, 084706 (2015).
- <sup>19</sup> Y. Song, C. Hellmann, N. Stingelin, and G. D. Scholes, *The Journal of Chemical Physics* **142**, 212410 (2015).
- <sup>20</sup> A. Bakulin and et al., *Nature Communications* **6**, 7880 (2015).
- <sup>21</sup> S. Pittalis, A. Delgado, J. Robin, L. Freimuth, J. Christoffers, C. Lienau, , and C. A. Rozzi, *Advanced Functional Materials* **25**, 2047 (2015).
- <sup>22</sup> P. Peumans and S. R. Forrest, *Chemical Physics Letters* **398**, 27 (2004).
- <sup>23</sup> S. N. Hood and I. Kassal, *The Journal of Physical Chemistry Letters* **7**, 4495 (2016).
- <sup>24</sup> A. A. Bakulin, A. Rao, V. G. Pavelyev, P. H. M. van Loosdrecht, M. S. Pshenichnikov, D. Niedzialek, J. Cornil, D. Beljonne, and R. H. Friend, *Science* **335**, 1340 (2012).



- <sup>25</sup> A. E. Jilaubekov, A. P. Willard, J. R. Tritsch, W.-L. Chan, N. S. Raluca Gearba, L. G. Kaake, K. J. Williams, K. Leung, P. J. Rossky, and X.-Y. Zhu, *Nature Materials* **12** (2013).
- <sup>26</sup> A. V. Akimov and O. V. Prezhdo, *Journal of the American Chemical Society* **136**, 1599 (2014).
- <sup>27</sup> R. A. Marsh, J. M. Hodgkiss, S. Albert-Seifried, and R. H. Friend, *Nano Letters* **10**, 923 (2010).
- <sup>28</sup> A.-M. Dowgiallo, K. S. Mistry, J. C. Johnson, and J. L. Blackburn, *ACS Nano* **8**, 8573 (2014).
- <sup>29</sup> E. Mårzell, A. Losquin, R. Svård, M. Miranda, C. Guo, A. Harth, E. Lorek, J. Mauritsson, C. L. Arnold, H. Xu, et al., *Nano Letters* **15**, 6601 (2015).
- <sup>30</sup> G. Spektor, D. Kilbane, A. K. Mahro, B. Frank, S. Ristok, L. Gal, P. Kahl, D. Podbiel, S. Mathias, H. Giessen, et al., *Science* **355**, 1187 (2017).
- <sup>31</sup> M. Shibuta, K. Yamamoto, T. Ohta, M. Nakaya, T. Eguchi, and A. Nakajima, *Scientific Reports* **6** (2016).
- <sup>32</sup> E. Runge and E. K. U. Gross, *Phys. Rev. Lett.* **52**, 997 (1984).
- <sup>33</sup> G. Onida, L. Reining, and A. Rubio, *Reviews of Modern Physics* **74**, 601 (2002).
- <sup>34</sup> C. A. Ullrich, *Time-Dependent Density-Functional Theory: Concepts and Applications* (Springer-Verlag, Berlin, Heidelberg, 2013).
- <sup>35</sup> N. T. Maitra, *Journal of Physics: Condensed Matter* (2017).
- <sup>36</sup> L. P. Kadanoff and G. Baym, *Quantum Statistical Mechanics* (Benjamin, New York, 1962).
- <sup>37</sup> G. Stefanucci and R. van Leeuwen, *Nonequilibrium Many-Body Theory of Quantum Systems* (Cambridge University Press; Cambridge, 2013).
- <sup>38</sup> K. Balzer and M. Bonitz, *Nonequilibrium Green's Functions Approach to Inhomogeneous Systems* (Benjamin, New York, 2013).
- <sup>39</sup> S. R. White, *Phys. Rev. Lett.* **69**, 2863 (1992).
- <sup>40</sup> G. De Chiara, M. Rizzi, D. Rossini, and S. Montangero, *Journal of Computational and Theoretical Nanoscience* **5**, 1277 (2008).
- <sup>41</sup> R. Pariser and R. G. Parr, *The Journal of Chemical Physics* **21**, 466 (1953).
- <sup>42</sup> J. A. Pople, *Trans. Faraday Soc.* **42**, 1375 (1953).
- <sup>43</sup> K. Ohno, *Theoretica chimica acta* **2**, 219 (1964).
- <sup>44</sup> K. S. Thygesen and A. Rubio, *Phys. Rev. Lett.* **102**, 046802 (2009).
- <sup>45</sup> P. Myöhänen, R. Tuovinen, T. Korhonen, G. Stefanucci, and R. van Leeuwen, *Physical Review B* **85**, 075105 (2012).
- <sup>46</sup> T. Holstein, *Annals of Physics* **8**, 325 (1959).
- <sup>47</sup> L. Hedin, *Phys. Rev.* **139**, A796 (1965).
- <sup>48</sup> J. B. Neaton, M. S. Hybertsen, and S. G. Louie, *Phys. Rev. Lett.* **97**, 216405 (2006).
- <sup>49</sup> K. Kaasbjerg and K. Flensberg, *Nano Letters* **8**, 3809 (2008).
- <sup>50</sup> N.-H. Kwong and M. Bonitz, *Phys. Rev. Lett.* **84**, 1768 (2000).
- <sup>51</sup> N. E. Dahlen and R. van Leeuwen, *Phys. Rev. Lett.* **98**, 153004 (2007).
- <sup>52</sup> P. Myöhänen, A. Stan, G. Stefanucci, and R. van Leeuwen, *EPL (Europhysics Letters)* **84**, 67001 (2008).
- <sup>53</sup> P. Myöhänen, A. Stan, G. Stefanucci, and R. van Leeuwen, *Phys. Rev. B* **80**, 115107 (2009).
- <sup>54</sup> M. P. von Friesen, C. Verdozzi, and C.-O. Almbladh, *Phys. Rev. Lett.* **103**, 176404 (2009).
- <sup>55</sup> M. Hopjan and C. Verdozzi, in *First Principles Approaches to Spectroscopic Properties of Complex Materials* (Springer Berlin Heidelberg, 2014), pp. 347–384.
- <sup>56</sup> P. Lipavský, V. Špička, and B. Velický, *Phys. Rev. B* **34**, 6933 (1986).
- <sup>57</sup> H. Haug and A.-J. Jauho, *Quantum Kinetics in Transport and Optics of Semiconductors* (Springer-Verlag, Berlin, 2007).
- <sup>58</sup> S. Hermanns, N. Schlünzen, and M. Bonitz, *Phys. Rev. B* **90**, 125111 (2014).
- <sup>59</sup> N. Schlünzen and M. Bonitz, *Contrib. Plasma Phys.* **56**, 5 (2016).
- <sup>60</sup> S. Latini, E. Perfetto, A.-M. Uimonen, R. van Leeuwen, and G. Stefanucci, *Phys. Rev. B* **89**, 075306 (2014).
- <sup>61</sup> G. Pal, Y. Pavlyukh, W. Hübner, and H. C. Schneider, *The European Physical Journal B* **79**, 327 (2011).
- <sup>62</sup> E. Perfetto, A.-M. Uimonen, R. van Leeuwen, and G. Stefanucci, *Physical Review A* **92**, 033419 (2015).
- <sup>63</sup> E. Perfetto, D. Sangalli, A. Marini, and G. Stefanucci, *Physical Review B* **92**, 205304 (2015).
- <sup>64</sup> D. Sangalli, S. Dal Conte, C. Manzoni, G. Cerullo, and A. Marini, *Phys. Rev. B* **93**, 195205 (2016).
- <sup>65</sup> E. A. A. Pogna, M. Marsili, D. De Fazio, S. Dal Conte, C. Manzoni, D. Sangalli, D. Yoon, A. Lombardo, A. C. Ferrari, A. Marini, et al., *ACS Nano* **10**, 1182 (2016).
- <sup>66</sup> D. Sangalli and A. Marini, *Europhysics Letters* **110**, 47004 (2015).
- <sup>67</sup> E. Perfetto, D. Sangalli, A. Marini, and G. Stefanucci, *Physical Review B* **94**, 245303 (2016).
- <sup>68</sup> Y. Bar Lev and D. R. Reichman, *Phys. Rev. B* **89**, 220201 (2014).
- <sup>69</sup> D. J. Luitz and Y. Bar Lev, *Ann. Phys. (Berlin)* p. 1600350 (2017).
- <sup>70</sup> E. Boström, M. Hopjan, A. Kartsev, C. Verdozzi, and C.-O. Almbladh, **696**, 012007 (2016).
- <sup>71</sup> K. Balzer, N. Schlünzen, and M. Bonitz, *Physical Review B* **94**, 245118 (2016).
- <sup>72</sup> F. Willaime and L. M. Falicov, *The Journal of Chemical Physics* **98**, 6369 (1993).
- <sup>73</sup> K. Aryanpour, D. Psiachos, and S. Mazumdar, *Phys. Rev. B* **81**, 085407 (2010).
- <sup>74</sup> T. G. Schmalz, L. Serrano-Andrés, V. Sauri, M. Merchán, and J. M. Oliva, *The Journal of Chemical Physics* **135**, 194103 (2011).
- <sup>75</sup> M. Dresselhaus, G. Dresselhaus, and P. Eklund, *Science of Fullerenes and Carbon Nanotubes: Their Properties and Applications* (Elsevier Science; San Diego, 1996).
- <sup>76</sup> J. You, F. Nori, and Y.-L. Lin, *Solid State Communications* **91**, 117 (1994).
- <sup>77</sup> M. Braga, S. Larsson, A. Rosen, and A. Volosov, *Astronomy and Astrophysics* **245**, 232 (1991).
- <sup>78</sup> A. I. Kuleff and L. S. Cederbaum, *Journal of Physics B: Atomic, Molecular and Optical Physics* **47**, 124002 (2014).
- <sup>79</sup> C. Lanczos, *Journal of Research of the National Bureau of Standards* **45**, 255 (1950).
- <sup>80</sup> P. Darancet, V. Olevano, and D. Mayou, *Phys. Rev. B* **81**, 155422 (2010).
- <sup>81</sup> M. Strange, C. Rostgaard, H. Häkkinen, and K. S. Thygesen, *Physical Review B* **83**, 115108 (2011).
- <sup>82</sup> C. Jin, M. Strange, T. Markussen, G. C. Solomon, and K. S. Thygesen, *The Journal of chemical physics* **139**, 184307 (2013).
- <sup>83</sup> E. Boström, A. Mikkelsen, and C. Verdozzi, *Physical Review B* **93**, 195416 (2016).